Bitlis Eren Üniversitesi Fen Bilimleri Dergisi
BİTLİS EREN UNIVERSITY JOURNAL OF SCIENCE
ISSN: 2147-3129/e-ISSN: 2147-3188
VOLUME: 13 NO: 4 PAGE: 896-904 YEAR: 2024
DOI: 10.17798/bitlisfen.1458956

Design, Fabrication, and Piezoelectric Performance Evaluation of a Nanogenerator for Vibrational Energy Harvesters

Levent PARALI[1*]

[1]*Manisa Celal Bayar University, Electronics & Automation Department, Turgutlu Vocational School, Manisa / Türkiye*
(ORCID: 0000-0002-4462-7628)

Keywords:
PVDF, PZT, Graphene, Electrospinning, Piezoelectric Nanogenerator Manufacturing, Energy Harvesting.

Abstract
In recent years, to provide power for wearable electronics, the mechanical energy obtained from environmental conditions through the piezoelectric nanogenerator into electricity has attracted interest. In this study, polyvinylidene fluoride (PVDF), lead zirconium titanate (PZT), and graphene nanoplatelets (GNP) based piezoelectric nanogenerators (PENs) were fabricated using electrospinning method. The experimental results evaluated using Thevenin's, Norton's, and the maximum power transfer theorems exhibited that the PVDF/PZT/GNP-based PEN had a 2.76 times greater electrical power efficiency (0.24 μW) at the resonance frequency of 20 Hz compared to that of the PEN based on the pure PVDF (0.09 μW) at the vibrational frequency of 25 Hz. The piezoelectric energy harvesters are highly suitable as self-powered wearable motion sensors because of the direct relationship between the vibration frequency and the generated output power.

1. Introduction

Although batteries are among the traditional power sources, they are limited in terms of power efficiency, energy storage capacity, power efficiency, and lifetime and require recurrent recharging. Therefore, recent advances in various small, mobility portable, remote-sensing, and low-power devices have increased the need for unconventional power sources [1]- [3]. As a result, in recent years there has been a significant increase in studies investigating energy harvesting devices as a preferred primary power source to bring down battery recharging and replacement costs and extend device life [4], [5]. For electronic devices used in sensor points [6], biomedical devices, health monitoring systems [7], and large-scale sensor networks [8], [9] that detect interactions at a distance, the use of energy harvesting devices can extend the lifetime of electronic devices and provide alternative specialized applications. Energy harvesting can be explained as the direct conversion of environmental energy sources such as mechanical, thermal, solar, bioenergy, hydropower, and wind into electrical energy using a specific material or transmission mechanism.

In order to convert human movement [10], mechanical vibration [11], water flow [12], etc. into electrical energy, piezoelectric nanogenerators commonly used in energy harvesting systems offer a simple and innovative approach. Flexible polymer piezoelectric nanogenerators (PENs) have been widely built as structured in different forms using polyvinylidene difluoride (PVDF) and its copolymers. The PVDF has five crystalline types (α, β, γ, δ, and Ɛ) depending on its chain conformation, the β and γ phases among crystalline types provide an advantage for the fabrications of actuators, sensors, batteries, and filters due to the fact that they have the greatest electrically active phases [13]-[14]. In order to enhance the β-phase transformation of PVDF, several approaches such as increasing the phase transition by applying a strong electric field [15], mechanical stretching [16], and the addition of nucleating fillers and particles [17], [18], etc. have been used in the literature.

Since the PZT ($Pb\ (Zr_xTi_{(1-x)})\ O_3$) ceramic particles have higher piezoelectric values and

*Corresponding author: levent.parali@cbu.edu.tr
Received: 26.03.2024, Accepted: 10.10.2024

mechanical properties, they are widely used in the fabrication of the PVDF/PZT-based piezoelectric nanogenerator [19], [20]. Recently, in order to further strengthen the connection between randomly dispersed ceramic particles in the polymer matrix (three-phase composite) and to improve the PVDF's β-phase, there has been a focus on the incorporation of some amount of filler (third conductive phase) such as carbon nanotubes (CNTs) [21], graphene particles (GNPs) [22], hydrated ionic salts [23], halides [24] into the polymer matrix.

This study aims to introduce the production of electrospun mats obtained through the electrospinning process, to show how they can be designed as a piezoelectric nanogenerator, and to determine their electrical performances using the vibrational energy harvesting system.

2. Material and Method

2.1. Materials

Polyvinylidene difluoride (PVDF) (MW: 534.000 g/mol, Alfa Aesar) was chosen as a polymer substrate while a PZT-5A (Navy Type II / APC 850, a particle size of < 1 μm) and Graphene Nanoplatelets (Nova Scientific Resources-M Sdn. Bhd.) were decided on doping materials respectively. Furthermore, N-dimethylformamide (DMF, Merck) (99.5%) and acetone (C3H6O, Merck) were used as chemical solvents.

2.2. Production of Electrospun Mat Through Electrospinning

The production stages of all electrospun mats are depicted in detail in Figure 1. The electrospinning method is a voltage-controlled producing process controlled by a specific electro-hydrodynamic phenomenon, to produce thin fiber mats from a polymer containing solutions. In this study, the initial sample consisted of pure PVDF, while the content of the second composite was built of the PVDF incorporated with the PZT and the pristine GNPs.

For the first specimen, the pure PVDF solution was constructed by dissolving PVDF powder (10% w/v) in a solvent consisting of a mixture of DMF and Acetone (DMF: 4.5 ml, Acetone: 10.5 ml) at 50 °C for 2 hours with magnetic stirring. On the other side, in order to dissolve GNPs in a weight ratio of 1.5wt.% in acetone, an ultrasonic mixing process was utilized for 3 hours, and then the PZT particles (15vol.%) were added to the GNP solution. All mixed solutions were stirred as additional by an ultrasonic and a magnetic stirrer for 5 hours again. Finally, the second sample solution was obtained by transferring the homogeneous PZT/GNP suspension to the PVDF solution and additional stirring for 5 h with a magnetic stirrer.

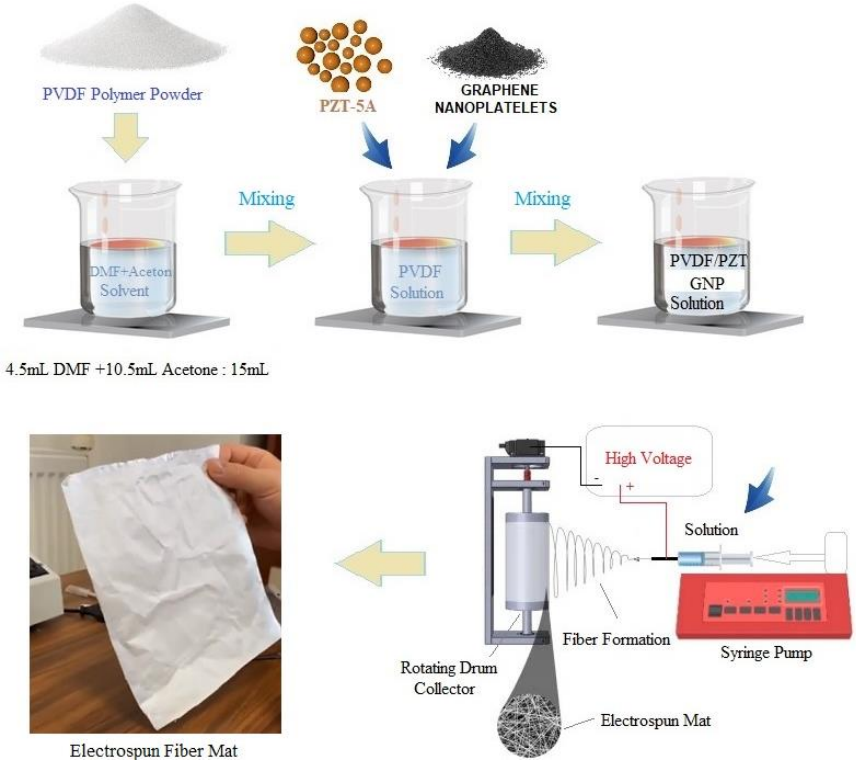

Figure 1. Production of the electrospun fiber mats using Electrospinning.

Consequently, the pure PVDF and the PVDF/PZT/GNP solutions were filled into the plastic syringe (diameter of syringe: 10 mL, a metallic needle with a 0.4 mm inner diameter), separately. The syringe was placed vertically on the pump, and the positive tip of the high-voltage supply was connected to the metal needle tip while the negative lead of the power supply was grounded. The rotation speed of the drum collector surrounded with aluminum sheet was 2400 rpm. When the solution was injected via a pump delivery rate of 4.0 mL/h into the rotating drum collector, the interval between the needle tip and the rotating drum collector was 15 cm. During solution injection, when the high-voltage supply value reached 15kV, the electrostatic force acted in the opposite direction, and the polymer solution at the Taylor cone was adhered as fiber form on the collector by overcoming the surface tension.

2.3. Fabrication of the PEN

In order to design a PEN device, an electrospun film cut to a size of 4 x 4 cm^2 was positioned between two conductive aluminum electrodes as shown in Figure 2. a.

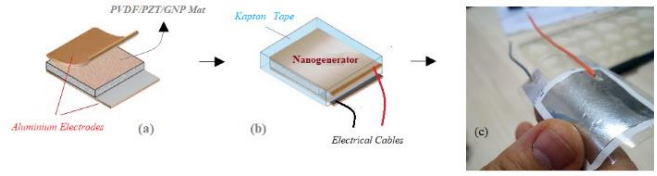

Figure 2. The fabrication stages of the piezoelectric nanogenerator.

Two copper cables were then attached to the surface of the aluminum electrodes on both sides with silver glue to ensure electrical conductivity. Afterward, as seen in Figure 2. b, the fabricated sample was fully protected by Kapton tape for a uniform packaging structure and finally obtained the flexible PEN device (Figure 2. c).

3. Results and Discussion

3.1. Structural Characterizations

The crystalline phase (X-Ray Diffraction, PANalytical Empyrean), Fourier-transform infrared spectroscopy (Bruker FTIR-ATR system), and morphology analyses (SEM: scanning electron microscopy, SUPRA 40VP) of the pure PVDF and the PVDF/PZT/GNP based fiber mats were shown Figures 3, 4, and 5 respectively as explained in detail in our previous study [25].

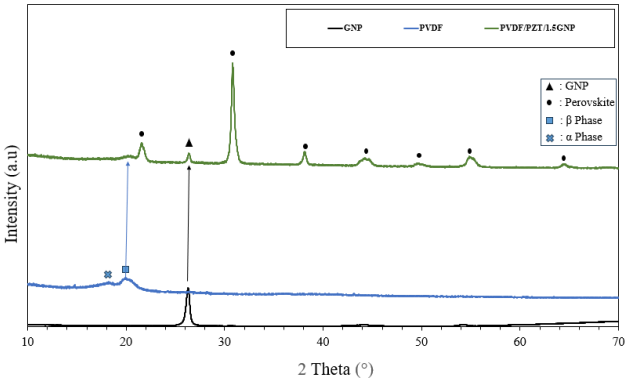

Figure 3. XRD Patterns of the neat PVDF and the PVDF/PZT/GNP with GNP loading concentration of 1.5wt.% [25].

According to Figure 3, the diffraction peak at 20.37° associated with the β phase, the characteristic diffraction peaks related to both the PZT (21.4°, 30.7°, 38°, 44.1°, 49.4°, 54.8°, and 64.4°) and the GNP (26.27°) exhibited the implementation of the electrospinning method in the formation of all samples remarkably reinforces the formation of the piezoelectric nanogenerator [25].

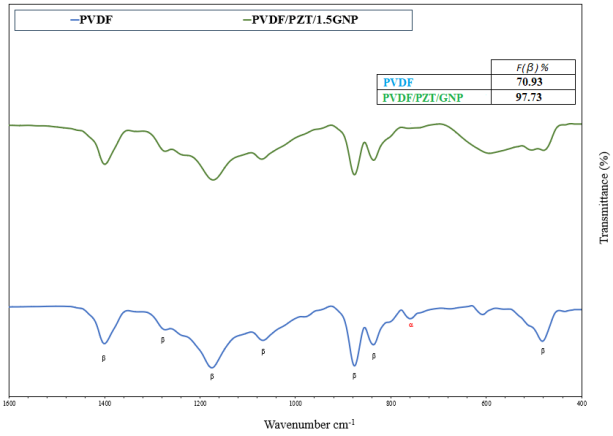

Figure 4. FTIR spectra of the pristine PVDF and the PVDF/PZT/1.5GNP [25].

When the FTIR spectra of all samples in Figure 4 are examined, it is deduced that the PEN based on the PVDF/PZT/1.5GNP reached the highest fraction of the β phase (97.73%) compared to the pristine PVDF (70.93%) [25]. Furthermore, the peaks (482°, 837°, 876°, 1068°, 1175°, 1272°, and 1400°) corresponding with the β phase shown in Figure 4 demonstrated an increase in the β phase formation of the composite structure [25]. As seen in SEM micrographs in Figure 5, it is observed that the PZT particles collected on fibers associated with the PVDF/PZT/GNP composite (Figure 5. b) due to the revolting force of the electric charges in contrast to the neat PVDF (Figure 5. a) [25].

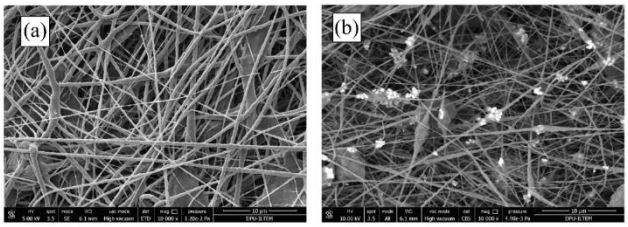

Figure 5. SEM images for the neat PVDF (a), the PVDF/PZT/1.5GNP electrospun mats (b) [25].

3.2. Electrical Performances of the PEN

In order to determine the electrical performances (voltage, current, and power) of the PEN device, Thevenin's, Norton's, and the maximum power transfer theorems were utilized through the two-terminal network system shown in Figure 6.

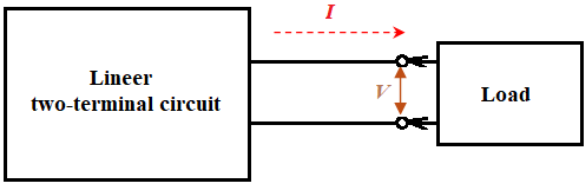

Figure 6. A linear two-terminal circuit.

Figure 7 indicates Thevenin's, Norton's, and the maximum power transfer equivalent circuits associated with the PEN.

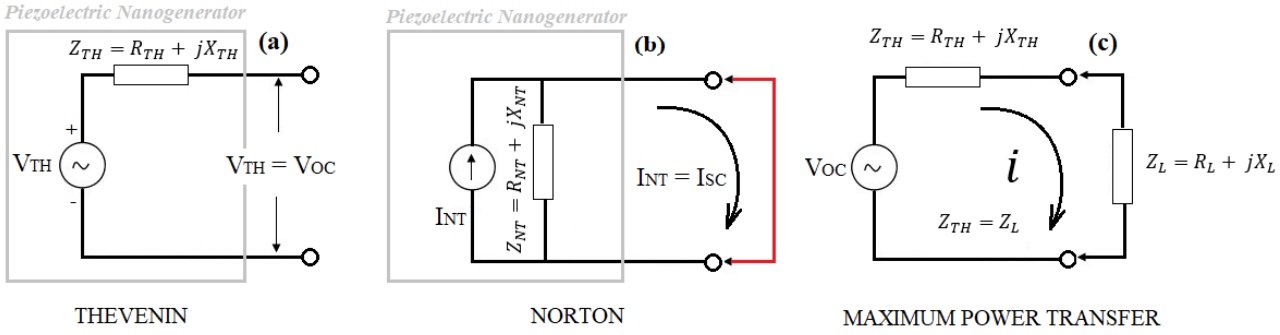

Figure 7. The Thevenin's (a), the Norton's (b), and the maximum power transfer (c) equivalent circuits of a PEN.

For AC circuit analysis, Thevenin's equivalent circuit consists of Thevenin's voltage-V_{TH} connected in series with Thevenin's impedance-Z_{TH} (Figure 7. a) while Norton's equivalent circuit contains Norton's current source-I_{NT} connected in parallel with Norton's impedance-Z_{NT} (Figure 7. b) [26]- [27].

As seen in Figure 7. a, if the terminals of the PEN device are open-circuited by removing the load impedance (Z_L), the open-circuit voltage between the terminals-V_{OC} will be equal to the voltage source V_{TH}, since no current is flowing in the circuit (V_{TH}=V_{OC}). When all independent sources are turned off, the input impedance-Z_i between the PEN tips will be equal to the Thevenin's impedance-Z_{TH} ($Z_i = Z_{TH}$).

According to Figure 7. b, when the PEN's tips are shorted, Norton's impedance-Z_{NT} will be shorted ($Z_{NT} = 0$) as well, hence Norton's current-I_{NT} equals a short circuit current-I_{SC} (I_{NT}=I_{SC}). If the independent energy sources are turned off, the input impedance-Z_i between the PEN terminals will be equal to Norton's impedance-Z_{NT} ($Z_i = Z_{NT}$).

As a result of all these explanations, considering the relationship between Thevenin's and Norton's theorems, we can write the following equation 1:

$$Z_{TH} = Z_{NT} = \frac{V_{OC}}{I_{SC}} \quad (1)$$

According to Figure 7. c, the electrical power on the load impedance (Z_L) can be expressed by the following equation 2:

$$P = i^2.Z_L = \left(\frac{V_{TH}}{Z_{TH}+Z_L}\right)^2.(Z_L) =$$

$$\left(\frac{V_{TH}}{R_{TH}+jX_{TH}+R_L+jX_L}\right)^2.(R_L + jX_L) \quad (2)$$

Due to the fact that the load resistance is a variable parameter, in order to find the maximum power, we differentiate the electrical power according to the load resistance, and this derivative must equal zero. After simplification, we get the below expressions.

$$X_L + X_{TH} = 0$$

$$X_L = -X_{TH}$$

It can be obtained from equation 3 by using the above relations [28].

$$\frac{dP}{dR_L} = V_{TH}^2 \left\{ \frac{(R_{TH}+R_L)^2 \frac{d}{dR_L}(R_L) - R_L \frac{d}{dR_L}(R_{TH}+R_L)^2}{(R_{TH}+R_L)^4} \right\} \quad (3)$$

$$\frac{dP}{dR_L} = V_{TH}^2 \left\{ \frac{(R_{TH}+R_L)^2 - 2R_L(R_{TH}+R_L)}{(R_{TH}+R_L)^4} \right\} = 0 \quad (3.1)$$

$$(R_{TH}+R_L)^2 - 2R_L(R_{TH}+R_L) = 0 \quad (3.2)$$

$$R_{TH} = R_L \quad (3.3)$$

From Eq.3.3, when Thevenin's resistance-R_{TH} is equal to the load resistance-R_L, it can be concluded that the maximum power will be transferred from the source to the load. Hence, we can achieve the equation. 4.1 via the equation. 4 [28].

$$P_{Max} = \left(\frac{V_{TH}}{R_{TH}+R_{TH}}\right)^2 . R_{TH} \quad (4)$$

$$P_{Max} = \frac{(V_{TH})^2}{4R_{TH}} = \frac{(V_{TH})^2}{4R_L} \quad (4.1)$$

We can also rewrite equation 1 as equation 5.

$$R_{TH} = \frac{V_{OC}}{I_{SC}} \quad (5)$$

Figure 8 depicts the experimental setup of the vibration energy harvesting system used to determine the piezoelectric performance of the PEN, which varies in proportion to the mechanical sensing performance, as well as several photographs of the manufactured PEN (Figure 8. a).

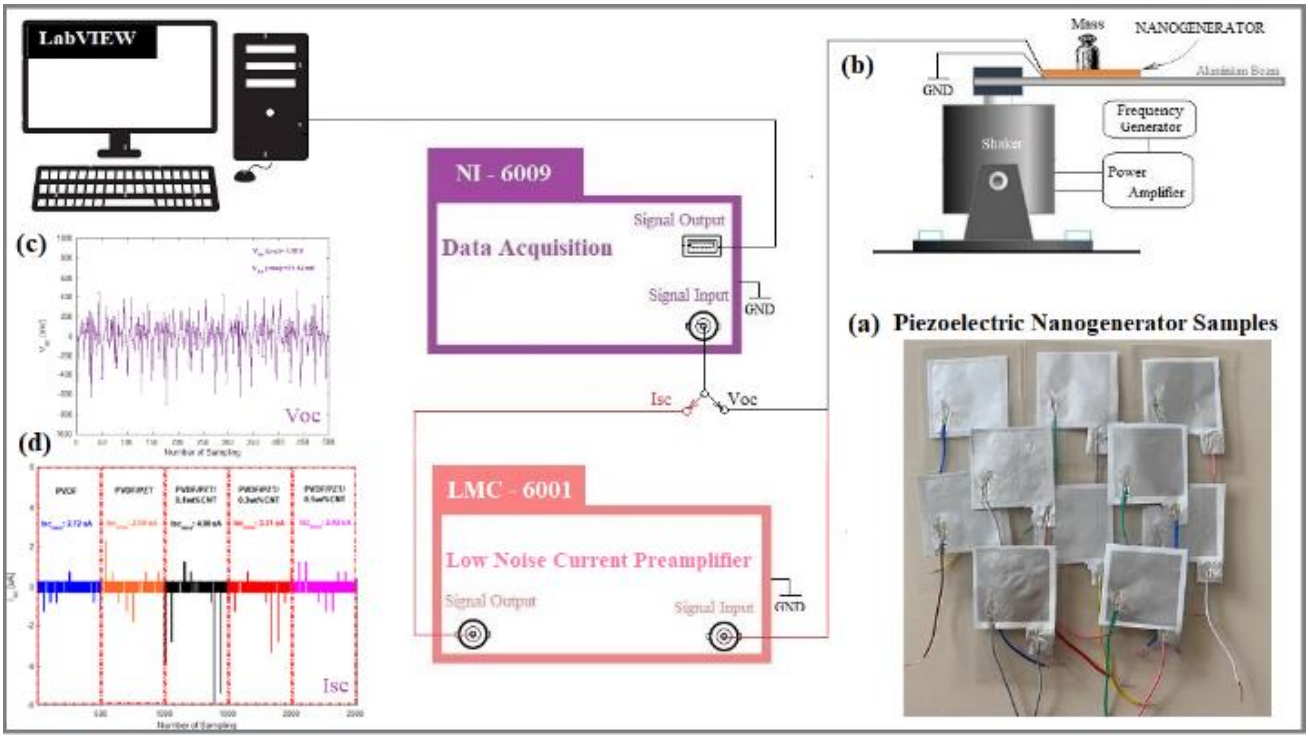

Figure 8. Vibrational energy harvesting system, and a photograph associated with fabricated PENs.

The vibrational energy harvesting system (Figure 8. b) is built of a magnetic shaker that vibrates an aluminum cantilever through a frequency signal generator at vibrational frequencies (5, 10, 15, 20, and 25 Hz). A power amplifier in the system provides a suitable amplitude for the efficient vibration of the magnetic shaker, whereas the NI-6009 and LMC-6001 data loggers are employed to measure the open-circuit voltage and the short-circuit current, respectively. Figures 8. c and d display the symbolic open circuit voltage-V_{OC} changes, and the symbolic short circuit current-I_{SC} changes.

The open circuit voltages (V_{OC}) all PEN samples were defined as V_{RMS} (RMS: the root-mean-square) by $V_{RMS} = \sqrt{\frac{1}{T}.\int_0^T Voc(t)^2 dt}$, while their

short-circuit currents (I_{SC}) were determined as I_{RMS} through $I_{RMS} = \sqrt{\frac{1}{T} \cdot \int_0^T Isc(t)^2 dt}$, where V_{RMS} = the effective voltage, the V_{OC} = the open-circuit voltage (V_{PP}: peak-to-peak), I_{RMS} = the effective short-circuit current, the I_{SC} = the short-circuit current (Isc_{PP}: peak-to-peak) and T = the periodic time.

The resonance (resonant) frequency is the characteristic frequency of a body or system that reaches the maximum degree of oscillation [29]. In the PEN devices, the resonant frequency is described by the vibration frequency at which the transfer function reaches its maximum voltage values. In this study, PEN devices were vibrated at specific frequencies (5, 10, 15, 20, and 25 Hz), and the maximum output voltage of the PEN was investigated at which frequency. Determining the resonant frequency of the PEN device is important in discovering the most efficient application range.

Figures 9 and 10 exhibit the V_{OC} and V_{RMS} changes of the PEN samples according to the vibrational frequencies (5, 10, 15, 20, and 25 Hz).

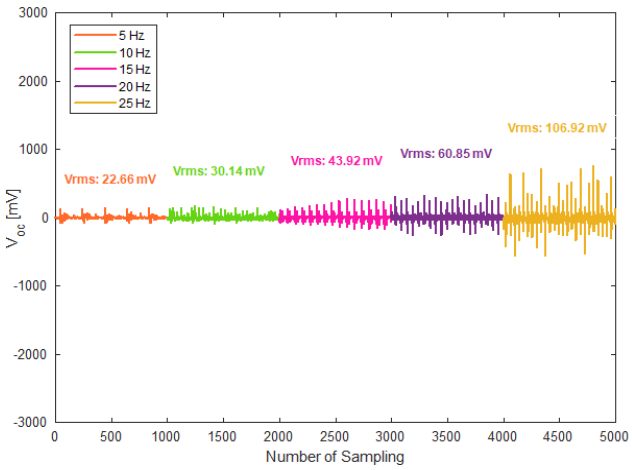

Figure 9. According to vibrational frequencies, the V_{OC} and V_{RMS} changes of the PEN based on the pure PVDF.

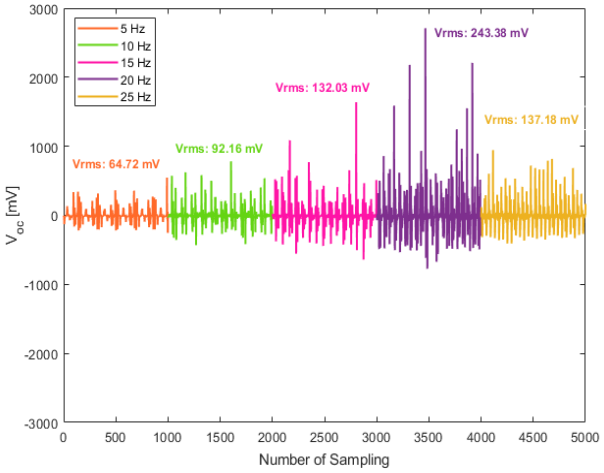

Figure 10. According to vibrational frequencies, the V_{OC} and V_{RMS} changes of the PEN based on the PVDF/PZT/GNP.

Figures 11 and 12 reveal the I_{SC} and the I_{RMS} alternates of all samples in compliance with the vibrational frequencies (5, 10, 15, 20, and 25 Hz).

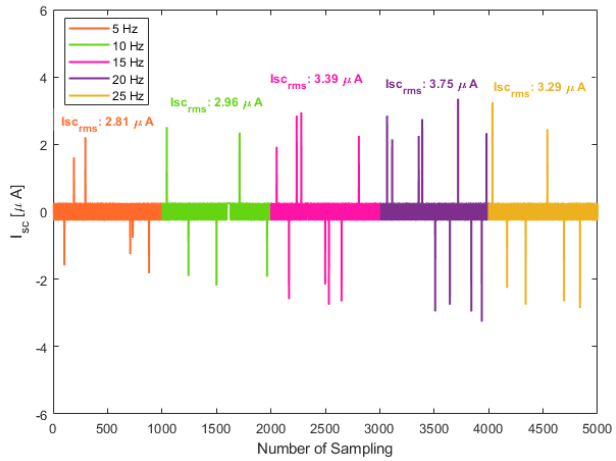

Figure 11. The I_{SC} and the I_{RMS} values depend on the vibrational frequency of the PEN based on the pure PVDF.

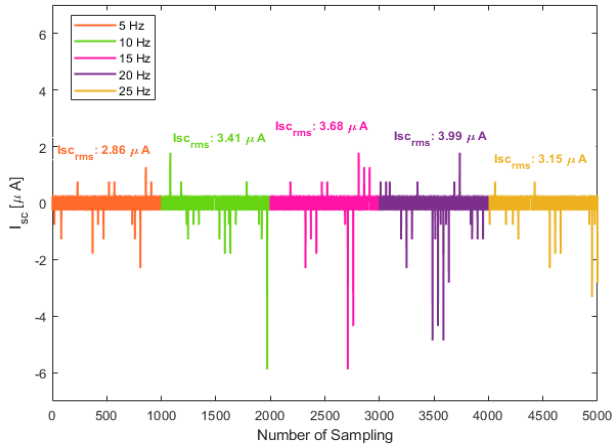

Figure 12. The I_{SC} and the I_{RMS} values depend on the vibrational frequency of the PEN based on the PVDF/PZT/GNP.

The maximum V_{RMS} value of 243.38 mV and I_{SC} value of 3.99 µA at 20 Hz for the PVDF/PZT/GNP electrospun mat-based PEN were measured as compared to the PEN based on the PVDF mat (V_{RMS}: 106.92 mV and I_{SC}: 3.29 µA at 25 Hz).

Figures 13 and 14 show the V_{RMS}, the I_{RMS}, and the P_{MAX} variations as a function of frequency for all samples.

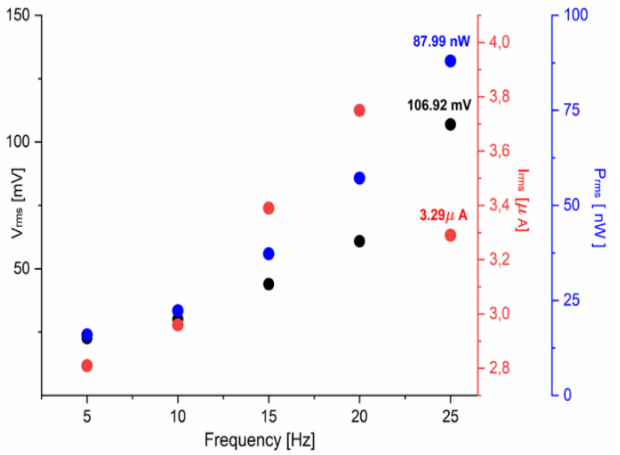

Figure 13. The V_{RMS}, the I_{RMS}, and the P_{RMS} changes of the PEN based on the pure PVDF.

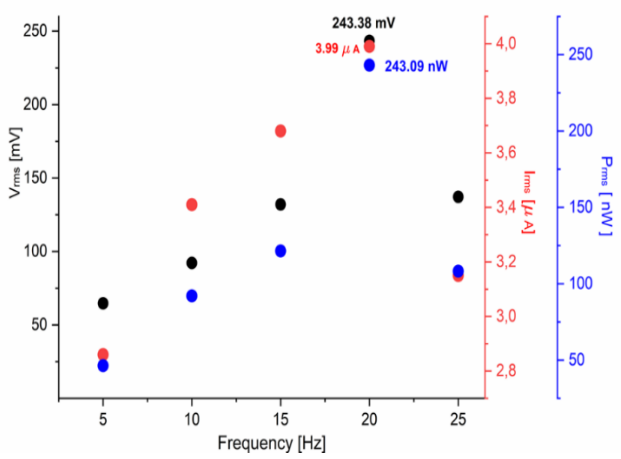

Figure 14. The V_{RMS}, the I_{RMS}, and the P_{RMS} changes of the PEN based on the PVDF/PZT/GNP.

According to Figure 15, in order to attitudes a general evaluation of samples, we can say that the fabricated PEN based on the PVDF/PZT/GNP reached an open circuit voltage of 0.24 V, and the highest electrical power of 0.24 µW by drawing a current of 1.99 µA at the vibrational frequency values of 20 Hz under a resistive load of 60.91 KΩ whereas the pure PVDF based PEN had 0.1 V, 1.64 µA, and 0.09 µW at the vibrational frequency values of 25 Hz under the resistive load of 32.48 KΩ, respectively.

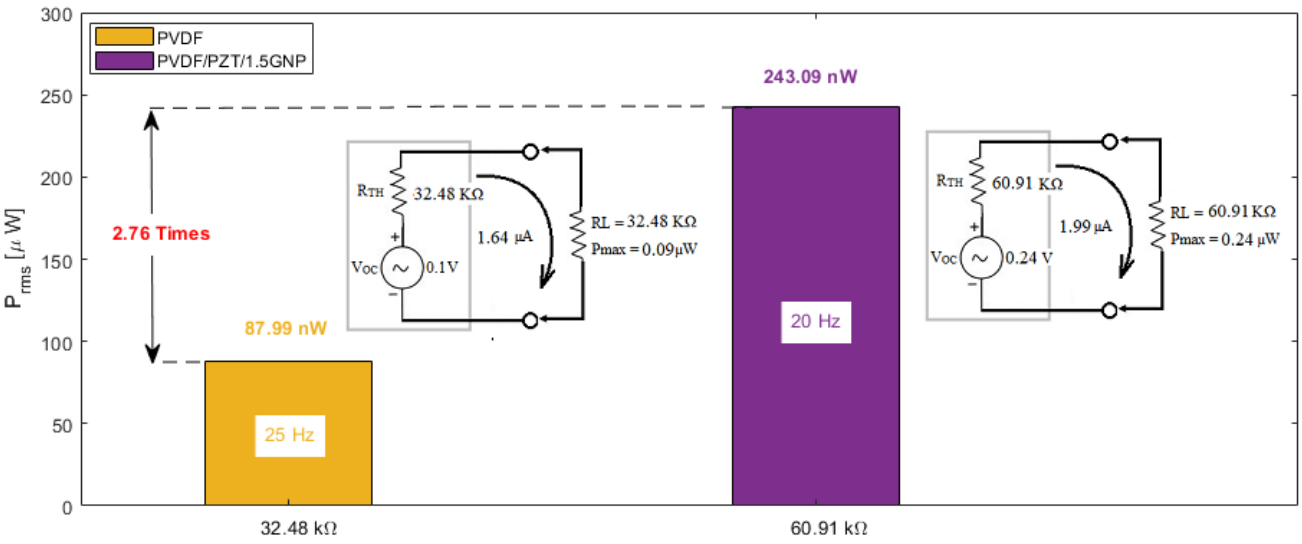

Figure 15. Comparing the $P_{MAX\text{-}RMS}$ alternations between the pure PVDF and the PVDF/PZT/1.5GNP.

In order to assess the stability and durability of the PVDF/PZT/1.5GNP-based piezoelectric energy harvester, a mechanical vibration test was performed under a vertical application force of 1 N at a frequency of 20 Hz.

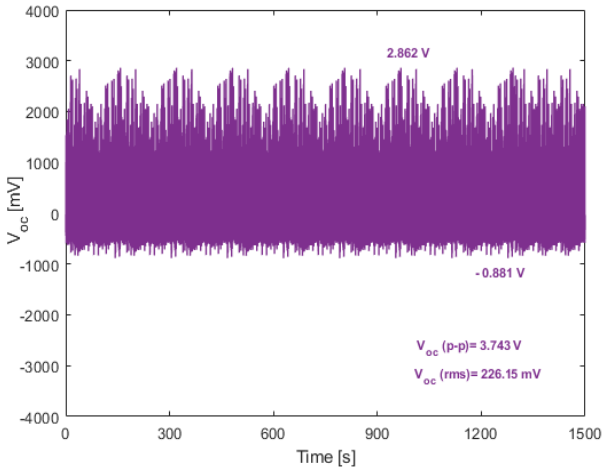

Figure 16. Stability test of the piezoelectric energy harvester for the 1500s.

It can be seen from Figure 16 that the output voltage alternations persisted almost stable for the 1500s, indicating the highest quality mechanical stability and durability.

4. Conclusion and Suggestions

The pure PVDF and the PVDF/PZT/GNP-based PENs were successfully fabricated through electrospinning. According to Thevenin's, Norton's, and the maximum power theorems, the PEN device based on the PVDF/PZT/1.5GNP which has the maximum open circuit voltage of 0.24 V (V_{RMS}) compared to the neat PVDF-based PEN, reached the highest power capacity of 243 nW (P_{RMS}) by drawing a current (I_{RMS}) of 1.99 μA at a vibrational frequency of 20 Hz (impact force of 1N) under a resistive load of 60.91 KΩ. In other words, the PEN based on the PVDF/PZT/1.5GNP had a better electrical power efficiency rate of 175% than that of the pure PVDF. Considering a microwatt-based energy harvesting system, the direct use of the PEN device is not enough for the energy harvesting system. Therefore, to boost the power transfer and minimize signal reflection (for better Signal/Noise ratio), it is mandatory to use a power management system that includes impedance matching, low & band-pass filters, a pre-amplifier, etc.

Statement of Research and Publication Ethics

The study is complied with research and publication ethics.

References

[1] R. Fazio, D. Cafagna, G. Marcuccio and P. Visconti, "Limitations and characterization of energy storage devices for harvesting applications", *Energies*, vol.13-4, 783, February 2020.

[2] A.Z.A. Shaqsi, K. Sopian and A. Al-Hinai, "Review of energy storage services, applications, limitations, and benefits", *Energy Rep*. vol. 6, pp. 288–306, 2020.

[3] A. Olabi, M.A. Abdelkareem, T. Wilberforce and E.T. Sayed, "Application of graphene in energy storage device–A review", *Renewable Sustainable Energy Reviews*, vol.135, 2021, 110026.

[4] R.A. Surmenev, R.V. Chernozem, I.O. Pariy and M.A. Surmeneva, "A review on piezo and pyroelectric responses of flexible nano-and micropatterned polymer surfaces for biomedical sensing and energy harvesting applications", *Nano Energy*, vol. 79, 2021, 105442.

[5] S.A. Graham, S.C. Chandrarathna, H. Panama, P. Manchi, J.-W. Lee and J.S. Yu, "Harsh environment–tolerant and robust triboelectric nanogenerators for mechanical-energy harvesting, sensing, and energy storage in a smart home", *Nano Energy*, vol.80, 2021, 105547.

[6] U. Yaqoob, S. M. I. Uddin and G.-S. Chung, "A Novel Tri-Layer Flexible Piezoelectric Nanogenerator Based on Surface- Modified Graphene and PVDF-$BaTiO_3$ Nanocomposites", *Applied Surface Science*, vol. 405, pp. 420-426, 2017.

[7] Y. Wu, et al., "A multi-mode triboelectric nanogenerator for energy harvesting and biomedical monitoring", *Nano Energy*, vol. 92, 2022, 106715.

[8] N. Piovesan, A.F. Gambin, M. Miozzo, M. Rossi and P. Dini, "Energy sustainable paradigms and methods for future mobile networks: a survey", *Computer Communications,* vol. 119, pp. 101–117, 2018.

[9] H. Li, K. Ota and M. Dong, "Energy cooperation in battery-free wireless communications with radio frequency energy harvesting", *ACM Transactions Embedded Computing Systems*, vol. 17, pp. 1-17, 2018.

[10] A. Ali, S. Iqbal and X. Chen, "Recent advances in piezoelectric wearable energy harvesting based on human motion: Materials, design, and applications", *Energy Strategy Reviews*, vol. 53, pp. 1-16, 2024.

[11] S. Bairagi, S. Islam, M. Shahadat, D.M. Mulvihill and W. Ali, "Mechanical energy harvesting and self-powered electronic applications of textile-based piezoelectric nanogenerators: A systematic review", *Nano Energy*, vol. 111, pp. 1-29, 2023.

[12] Z. Li, J. Roscow, H. Khanbareh, G. Haswell and C. Bowen, "Energy Harvesting from Water Flow by using Piezoelectric materials ", *Advanced Energy & Sustainability Research*, vol. 5, pp. 1-33, 2024.

[13] A. Salimi and A.A. Yousefi, "Analysis Method: FTIR studies of beta-phase crystal formation stretched PVDF films ", *Polymer Testing*, vol. 22, pp. 699-704, 2003.

[14] H. Pan, B. Na, R. Lv, C. Li, J. Zhu and Z. Yu, "Polar phase formation in poly (vinylidene fluoride) induced by melt annealing", *Journal of Polymer Science, Part B: Polymer Physics*, vol.50, pp. 1433–1437, 2012.

[15] S.F. Mendes, C.M. Costa, C. Caparros, V. Sencadas and S. Lanceros-Mendez, "Effect of filler size and concentration on the structure and properties of poly (vinylidene fluoride)/$BaTiO_3$ nanocomposites", *Journal of Materials Science*, vol. 47, pp. 1378–1388, 2012.

[16] Y. Wang, D. Lei, L. Wu, R. Ma, H. Ning, N. Hu and A. Lee, "Effects of stretching on phase transformation of PVDF and its copolymers: A review", *Open Physics*, vol. 21, 2023, 2022-0255.

[17] R.S. Sabry and A.D. Hussein, "PVDF: ZnO/$BaTiO_3$ as high out-put piezoelectric nanogenerator", *Polymer Testing*, vol. 79, 2019, 106001.

[18] H.G. Yeo, X. Ma, C. Rahn and S. Trolier-McKinstry, "Efficient piezoelectric energy harvesters utilizing (001) textured bimorph PZT films on flexible metal foils", *Advanced Functional Materials* vol.26, pp. 5940–5946, 2016.

[19] X. Chen, S. Xu, N. Yao and Y. Shi, "1.6 V nanogenerator for mechanical energy harvesting using PZT nanofibers", *Nano Letter*, vol. 10, pp. 2133–2137, 2010.

[20] M. Sobocinski, M. Leinonen, J. Juuti, N. Mantyniemi and H. Jantunen, "A co-fired LTCC–PZT monomorph bridge type acceleration sensor", *Sensors and Actuator A: Physical*, vol. 216, pp. 370–375, 2014.

[21] X. Lin, F. Yu, X. Zhang, W. Li, Y. Zhao, X. Fei, Q. Li, C. Yang, and S. Huang, "Wearable Piezoelectric Films Based on MWCNT-$BaTiO_3$/PVDF Composites for Energy Harvesting, Sensing, and Localization", *ACS Applied Nano Materials*, vol. 6, pp. 11955−11965, 2023.

[22] R. Sridar, V. Amith, S. Aditva, A. Gangadhar and K.A. Vishnumurthy, "Electrospun PVDF/Cloisite-30B and PVDF/$BaTiO_3$/graphene nanofiber mats for development of nanogenerator", Journal of the Indian Chemical Society, vol. 99, 2022, 100501.

[23] S. K. Ghosh, A. Biswas, S. Sen, C. Das, K. Henkel, D. Schmeisser and D. Mandal, "Yb3+ assisted self-polarized PVDF based ferroelectric nanogenerator: A facile strategy of highly efficient mechanical energy harvester fabrication", Nano Energy, vol. 30, pp. 621-629, 2016.

[24] L. H. Meng, C. Yang, J. Meng, Y. Wang, Y. Ge, Z. Shao, G. Zhang, A. L. Rogach and H. Zhong, "In-situ fabricated anisotropic halide perovskite nanocrystals in polyvinyl alcohol nanofibers: Shape tuning and polarized emission", *Nano Research*, vol. 12, pp. 1411-1416, 2019.

[25] L. Paralı, F. Tatardar, M. Koç, A. Sarı and R. Moradi, "The piezoelectric response of electrospun PVDF/PZT incorporated with pristine graphene nanoplatelets for mechanical energy harvesting", *Journal of Materials Science: Materials in Electronics*, vol. 35, 41, 2024.

[26] John Hiley, Keith Brown and Ian McKenzie Smith, "Electrical and Electronic Technology", 10th edition, Pearson Education Limited, 2008.

[27] Alexander, Charles K., and Sadiku, Matthew N. O., "Fundamentals of Electric Circuits", 5th Ed, McGraw Hill, Indian Edition, 2013.

[28] Md. Abdus Salam and Quazi Mehbubar Rahman, "Fundamentals of Electrical Circuit Analysis", ISBN 978-981-10-8624-3 (eBook), Springer Nature Singapore Pte Ltd. 2018.

[29] David Halliday, Robert Resnick and Jearl Walker, "Fundamentals of Physics", 7th Ed, ISBN 978-0-471-71716-4, John Wiley & Sons Limited, 2005.